

International Journal of Applied Mathematics in Control Engineering

Journal homepage: <http://www.ijamce.com>

Multivariate Spline over Sectorial Partition

Jincai Chang^{*}, Mengyao Bao, Yafei Zhu, Xiaolong Zhang, Yajing Qi*School of Science, North China University of Science and Technology, Tangshan, Hebei, 063009, China*

ARTICLE INFO

Article history:

Received 25 August 2018

Accepted 30 October 2018

Available online 25 December 2018

Keywords:

Smoothing cofactor

Spline of revolution

Partition of concentric circles

Partition of spiral

ABSTRACT

Starting from univariate truncated spline, continuous and discontinuous spline surfaces are obtained by rotating for the center with an endpoint of spline, and two kinds of partition form of spline surface are presented. In order to get the unified partition form of spline surface, by changing the position of the pivot point and making the spline surface rotate along one point outside the domain, the improved spline surface is obtained eventually. Furthermore, by promoting the improved form of spline partition, the general expression of spline surface based on the partition of concentric circles $s(r, \theta) \in S_k^u(\Delta_{mm})$ is set up. At the same time, the expression of partition surface is more concise by partitioning in spiral, and provides tools for complex surface modeling.

Published by Y.X.Union. All rights reserved.

1. Introduction

Spline function, or spline for short, is a piecewise polynomial. The polynomials between adjacent slices have some sort of connection properties. Thus spline not only maintains the simplicity of polynomial and the feasibility of approximation, but also keeps relatively independent local property between each piece. In 1946, Schoenberg I. J. studied univariate spline function systematically^[1]. Since multivariate splines rely heavily on the geometric properties of domain decomposition, it presents a very complex situation. Regarding the study of multivariate spline functions, different types have emerged due to differences in use.

In 1963, the tensor product of the univariate splines is tried, as a result of certain conditionality of multivariate splines control vertices, the control surface cannot be well demonstrated^[2]. In 1975, by means of Bezout's theorem in algebraic geometry, a basic theoretical frame of multivariate spline for any partition is established and smooth cofactor method is proposed by professor Wang^[3]. With the help of this method, any problem on multivariate splines could be essentially equivalent to a corresponding algebraic problem. In 1976, Duchon^[5] derived the interpolation method of the thin plate spline function by starting from the theory that thin plate bending energy is the smallest, and realized the so-called "Thin-plate spline" in the two-dimensional case. In essence, thin plate spline is not spline function in the sense of piecewise polynomial, but a radial basis function. A spline with a partial polynomial partial division is called a mesh spline. This article

refers to a thin plate spline as a meshless spline. In 2007, the mechanical model of bivariate splines over some special partition was set up by professor Wang et al., and made the bivariate splines has the meaning of mechanics, that is, a deflection surface of bending of thin plate under the action of suitable load on the split line^[6,8]. Due to the grid and meshless splines are the generalizations of univariate splines, Wu Zongmin^[9] put forward the following conjecture: in the sense of mechanics, multivariate grid splines and meshless splines are unified, both can convert each other. To investigate the relationship between two types of spline, this paper discusses the conversion of grid and meshless spline on circular sector partition.

The structure of this paper is as follows: The second section introduces the existence theorem and expression of the binary grid splines. In Section 3, we give the multivariate splines surface by the rotating of univariate spline, and point out that the partition of rotation spline surface is concentric ring. At last, the form of rotation spline partition is extended to give a sectorial partition, and the general expression of multivariate spline over sectorial partition is presented in Section 4.

2. Theoretical Analysis of Univariate Spline Function

The spline function is essentially a piecewise polynomial with a certain degree of smoothness. The polynomial on each adjacent segment has some kind of connection property, so it not only keeps the simplicity of the polynomial and the feasibility of approximation, but also the relatively independent local properties are maintained

* Corresponding author.

E-mail addresses: jincail@ncst.edu.cn(J. Chang)

between segments. Spline functions are widely used in many fields such as function approximation, data analysis, finite element and computational geometry.

2.1 Bernstein-Bézier curve

1962 Renault engineer the Bézier put forward a kind of simple and easy to use by the control polygon defined curve modelling method, push forward the curve surface design, laid a good foundation for surface modeling.

2.1.1 Bernstein polynomial

A function $f(x) \in C[0,1]$ the Bernstein polynomial is defined

$$B_v^\varphi[\xi] = \sum_{i=0}^v \varphi\left(\frac{t}{v}\right) B_i^v, 0 \leq \xi \leq 1 \tag{2-1}$$

where

$$B_i^n(x) = \binom{n}{i} x^i (1-x)^{n-i} \quad i = 0, 1, 2, \dots, n; 0 \leq x \leq 1$$

$\{B_i^n(x)\}_{i=0}^n$ is Linearly independent, a set of base for P_n . Each function $B_i^n(x) (i = 0, 1, \dots, n)$ is called basis functions of Bernstein.

2.1.2 Bézier curve

Define a curve of degree n :

$$P(x) = \sum_{i=0}^n P_i B_i^n(x), 0 \leq x \leq 1 \tag{2-2}$$

where, P_i is referred to as control vertices. Control the adjacent vertices connected by straight line of polygon after referred to as the control polygon.

2.2 B-spline function

The B-spline is a generalization of the Bézier curve. The B-spline method inherits the advantages of the Bézier method and overcomes its shortcomings. It can directly obtain the approximation function, which solves the local control problem well.

2.2.1 B-spline basis function

The unary B-spline basis function has many different definition forms. For example, the pyramid algorithm gives a definition form from the relationship of each step basis function, which is more visual and intuitive; the B-spline defined by the truncated power function is more convenient in theory. Analysis of B-splines; but more internationally, the B-spline recursive definitions given by de Boor and Cox, which make B-splines more widely used in computer-aided geometric design. The de Boor-Cox recurrence formula is given below:

$$N_{i,0}(x) = \begin{cases} 1, & x \in (t_i, t_{i+1}) \\ 0, & x \notin (t_i, t_{i+1}) \end{cases}$$

$$N_{i,k}(x) = \frac{x-t_i}{t_{i+k}-t_i} N_{i,k-1}(x) + \frac{t_{i+k+1}-x}{t_{i+k+1}-t_{i+1}} N_{i+1,k-1}(x), k > 0$$

It can be seen from equation that any k-degree B-splines can be

linearly represented by adjacent k-1-degree B-splines.

According to the recursive formula of the B-spline basis function, two adjacent quadratic B-spline basis functions $N_{i,2}(u), N_{i+1,2}(u)$ can be obtained to obtain a cubic B-spline $N_{i,3}(u)$, as shown in the figure.

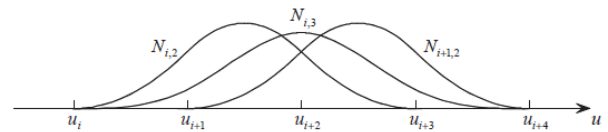


Fig 1 Cubic B-splines

If the segmentation of the node is uniform, then the basis function is called a uniform B-spline, and the images on the respective node intervals in the definition domain are the same, which is equivalent to the translation of the image of the other node interval.

2.2.2 B-spline curve

Given $n+1$ control fixed points b_i (also known as de Boor control points) ($i = 0, 1, \dots, n$), is the k degree B-spline basis function defined on the node vector $U = [u_0, u_1, \dots, u_{n+k+1}]$, then the k-order B-spline curve is

$$P(u) = \sum_{i=0}^n d_i N_{i,k}(u), u \in [u_i, u_{i+1}] \subset [u_k, u_{n+1}]$$

The polyline connected in order by the control fixed point $N_i, i = 1, \dots, V$ becomes a B-spline control polygon.

In particular, when $N_{i,k}(x), x \in [0,1]$, $d_k^u(N)$ represents k degree uniform B-spline basis function. $V_i(x) (i = 0, 1, \dots, k)$, represents the vertices of the control polygon, then a k degree uniform B-spline curve can be expressed as

$$p(x) = \sum_{i=0}^k N_{i,k}(x) V_i(x), x \in [0,1] \tag{2-3}$$

3. Basic Theorem of Multivariate Spline and Bending of Thin Plate

3.1 Truncated spline function

Given a set of nodes

$$-\infty = x_0 < x_1 < \dots < x_N < x_{N+1} = \infty$$

Let the piecewise function $S(x)$ satisfy

(1) For each interval $[x_j, x_{j+1}] (j = 0, \dots, N)$, $S(x)$ is an algebraic polynomial of real coefficients of no more than n .

(2) $S(x)$ has a continuous derivative up to the order $n-1$, so

$y = S(x)$ is called n degree spline function. It's often called the population of then degrees spline function. x_1, \dots, x_N is called the spline node.

The expression of $S(x)$ is

$$S(x) = p_n(x) + c_1 (x-x_1)_+^n, \quad (-\infty \leq x \leq x_2) \tag{3-1}$$

where

$$x_+ = \max(0, x) = \begin{cases} x & x > 0 \\ 0 & x \leq 0 \end{cases}, \quad x_+^m = (x_+)^m$$

3.2 Smoothing cofactor method for multivariate splines

Let D be a domain in R^2 , and p_k be the collection of all the bivariate polynomials with real coefficients and total degree $\leq k$. A bivariate polynomial P is called irreducible polynomial, If and only if it can be completely divisible by the constant and polynomial itself and there is no other complex polynomial. Irreducible algebraic curve is defined by

$$\Gamma : l(x, y) = 0, l(x, y) = P_k R^2 \tag{3-2}$$

where $l(x, y)$ is irreducible polynomial.

Using a finite number of irreducible algebraic curves to carry out the partition Δ , we divide the domain D into a finite number of sub-domains D_1, \dots, D_N , each of the sub-domains is called a cell. The line segments forming the boundary of each element are called "edges"; the intersections of the edges are called "vertices"; the two vertices of the same side are called "adjacent vertices". The sets of cells with the vertices of V are called "associated domains or astral domains", denoted by $St(V)$. The space of multivariate spline functions is defined by

$$S_k^\mu(\Delta) = \{s \in C^\mu(D) : s|_{D_i} \in P_k, i = 1, \dots, N\} \tag{3-3}$$

where s is a piecewise polynomial of degree k possessing μ order continuous partial derivatives in D . Based on the Bezout's theorem of algebraic geometry, Wang^[2] got the smoothing connection conditions of multivariate splines, shown as the following theorem:

Theorem 3.1 Let $s \in S_k^\mu(\Delta)$, D_i and D_j are two arbitrary adjacent cells of the partition Δ . If irreducible algebraic curve $\Gamma : l(x, y) = 0$ is a common interior edge of D_i and D_j , $P_i = s|_{D_i}, P_j = s|_{D_j}$, then there is

$$P_i - P_j = (l(x, y))^{\mu+1} q(x, y) \tag{3-4}$$

where $q(x, y) \in P_{k-(\mu+1)d}$, $d = \deg(l)$ is called the smoothing cofactor on irreducible algebraic curve Γ .

Theorem 3.2 Let Δ be any partition of D , the multivariate spline function $s(x, y) \in S_k^\mu(\Delta)$ exists, if and only if for every interior edge, there exists a smoothing cofactor, which satisfies the global conformality condition

$$\sum_{i=1}^N (l_i(x, y))^{\mu+1} q_i(x, y) = 0$$

at each interior mesh point.

Theorem 3.3 Any $s \in S_k^\mu(\Delta)$ can be uniquely represented as follows:

$$s(x, y) = p(x, y) + \sum_C (l_{ij}(x, y))_*^{\mu+1} q_{ij}(x, y), (x, y) \in D \tag{3-5}$$

where $p(x, y) \in P_k$ is the expression of $s(x, y)$ in the source cells, \sum_C .

3.3 Multi-spline function space on the cross-cut partition

If the partition Δ of the region D is formed such that all of its mesh lines are cut by a straight line penetrating the region D . Then, such a partition Δ is "cross-cut partition".

Let Δ_c have L cross-cut lines in D, V interior mesh points A_1, \dots, A_V and n_i cross-cut lines intersect $A_i, i = 1, \dots, V$.

Let $(\alpha_1, \beta_1), \dots, (\alpha_N, \beta_N)$ be pairwise linearly independent ordered pairs, that is, $\alpha_i \beta_j \neq \alpha_j \beta_i, i \neq j, i, j = 1, \dots, N$, and V_N be the solution vector space corresponding to the conformality condition at a point.

$$V_N := \left\{ (q_1, \dots, q_N) \mid \sum_{i=1}^N q_i(x, y) (\alpha_i x + \beta_i y)^{\mu+1} \equiv 0 \right\} \tag{3-6}$$

Lemma 3.4 gives the $\dim V_N$ specific formula.

Lemma 3.4

$$\dim V_N =: d_k^\mu(N) =: \frac{1}{2} \left(k - \mu - \left[\frac{\mu+1}{N-1} \right] \right)_+ \cdot ((N-1)k - (N+1)\mu + (N-3)) \cdot (N-1) \left[\frac{\mu+1}{N-1} \right]$$

Theorem 3.5

$$\dim S_k^\mu(\Delta_c) = \binom{k+2}{2} + L \binom{k-\mu+1}{2} + \sum_{i=1}^V d_k^\mu(n_i) \tag{3-8}$$

where L cross-cuts, n_i cross-cuts intersect at $A_i, i = 1, \dots, V, V$ interior mesh points.

Theorem 3.6 Let Δ_{qc} be a quasi-cross partition of simply connected region. Δ_{qc} has L_1 cross-cuts and L_2 rays. Let Δ_{qc} have V interior mesh points A_1, \dots, A_V , and $N_i, i = 1, \dots, V$ cross-cuts and rays passing through A_i .

We have

$$\dim S_k^\mu(\Delta_{qc}) \binom{k+2}{2} + L_1 \binom{k-\mu+1}{2} + \sum_{i=1}^v d_k^\mu(N_i)$$

where $d_k^\mu(N)$ is given by Lemma (3-8).

Define the bivariate spline functions as

$$S_{i,j,t} = \sum_{s=1}^{m(i,j)} q_{i,j}(x,y) [l_{i,j}(x,y)]^{\mu+1}$$

where $q_{i,j}(x,y) \in P_{k-\mu+1}$.

Clearly $S_{i,j,t} \in S_k^\mu(\Delta_c), t=1, \dots, d_k^\mu(m(i,j))$ and are supported in the angle measured counterclockwise from $l_{i,j,1}$ to $l_{i,j,m(i,j)}$.

Theorem 3.7 The collection of bivariate splines

$$B := \left\{ \begin{array}{l} S_{i,j,t}(x,y), x^a y^b x^c y^d \\ \left. \begin{array}{l} 0 \leq a+b \leq k \\ 0 \leq c+d \leq k-\mu-1 \\ \mu=1, \dots, L \\ t=1, \dots, d_k^\mu(m(i,j)) \\ j=1, \dots, m_i \\ i=1, \dots, L \end{array} \right\} \right. \quad (3-10)$$

is a basis of $S_k^\mu(\Delta_c)$.

3.4 Elasticity and plate bending

The equilibrium differential equation for the bending of elastic thin plates was obtained in 1811 by Lagrange in reviewing the research report on plate bending sent by Sophie Germain to the French Academy of Sciences. The bending properties of the plate largely determine its thickness. We only discuss the bending of the thin plate with small deflection. Within the framework of the elastic theory, the thin deflection theory of thin plates has the following basic assumptions:

(1) The middle surface of the plate is not deformed and remains neutral when bent;

(2) The straight line perpendicular to the middle surface of the plate before the bending deformation is still perpendicular to the deformed middle curved surface after the deformation, and the length of the line segment remains unchanged. The straight normal line is assumed, and the deflection w is independent of z at this time, is only a function of two coordinates x and y in the plane of the board, ie $w = w(x, y)$;

The lateral normal stress of the plate is much smaller than other stresses and can be ignored. This hypothesis completely optimises the material properties and permits the use of a stress-strain relationship expressed by two elastic constants E and ν . Based on the above assumptions, an effective approximation theory of plate bending is established.

Under the above ideal assumption, the plate bending problem is attributed to solving a fourth-order differential equation, that is, the equilibrium equation.

$$\frac{\partial^4 w}{\partial x^4} + 2 \frac{\partial^4 w}{\partial x^2 \partial y^2} + \frac{\partial^4 w}{\partial y^4} = \frac{q}{D} \quad (3-11)$$

where the lateral load $q = q(x, y)$ represents the lateral load concentration perpendicular to the board surface. The general solution of the above fourth-order differential equation will have eight arbitrary constants. For a rectangular plate, each boundary should have two independent boundary conditions to determine the eight unknown constants. We briefly introduce the boundary conditions involved in practise.

Simple support: there is no deflection and no bending moment on the simple support edge. Therefore, if $x = a$ is a simple support edge, then there is

$$\begin{cases} w|_{x=a} = 0 \\ M_x|_{x=a} = -D \left(\frac{\partial^2 w}{\partial x^2} + \nu \frac{\partial^2 w}{\partial y^2} \right)_{x=a} = 0 \end{cases} \quad (3-12)$$

And because along the edge line $x = a, x = 0$, the change of the deflection w along the y -axis along the edge is equal to zero, that is

$$\frac{\partial w}{\partial y} = \frac{\partial^2 w}{\partial y^2} = 0$$

So the simple boundary condition can be written as

$$\begin{cases} w|_{x=a} = 0 \\ \left(\frac{\partial^2 w}{\partial x^2} \right)_{x=a} = 0 \end{cases} \quad (3-13)$$

Fixed edge: When the edge $x=a$ is fixed, the deflection on the side line and the slope of the middle surface are 0, which is

$$\begin{cases} w|_{x=a} = 0 \\ \left(\frac{\partial w}{\partial x} \right)_{x=a} = 0 \end{cases} \quad (3-14)$$

Free edge: If the edge $x=a$ is completely free, there is no bending moment and torque on the edge, and there is no vertical shear force, therefore

$$(M_x)_{x=a} = 0, (M_{xy})_{x=a} = 0, (Q_x)_{x=a} = 0 \quad (3-15)$$

The latter two conditions can be combined into one, ie torque and shear can be combined into equivalent shear

$$V_x = \left(Q_x - \frac{\partial M_{xy}}{\partial y} \right)_{x=a} = 0 \quad (3-16)$$

Therefore, the free boundary condition is

$$\begin{cases} M_x|_{x=a} = -D \left(\frac{\partial^2 w}{\partial x^2} + \nu \frac{\partial^2 w}{\partial y^2} \right)_{x=a} = 0 \\ V_x|_{x=a} = -D \left[\frac{\partial^3 w}{\partial x^3} + (2-\nu) \frac{\partial^3 w}{\partial x \partial y^2} \right]_{x=a} = 0 \end{cases} \quad (3-17)$$

3.5 Rectangular partitioning

Starting with a given spline, there are usually two ways to generate a spline surface. The first method is a rectangular partition, and the second method is a rotation method of a spline. This section briefly introduces the rectangular partitioning, and the fourth section focuses on the rotation of the spline surface.

When generating spline functions by using the method of rectangular partitioning, it can be divided into uniform rectangular partitions and non-uniform rectangular partitions. Here, we only need to briefly introduce the general situation of rectangular partitions.

Generally, for any size rectangular plate, it has any rectangular partition, as shown in Fig2. Let us consider a 3x3 square plate and ignore the unit of measure.

where $a > 0, b > 0, c > 0, d > 0$ such that

$$\begin{aligned} M_{cx} &= M_{x1} + M_{x2}, & M_{cy} &= M_{y1} + M_{y2} \\ M_{x2} &= 2M_{x1}, & M_{y2} &= 2M_{y1} \end{aligned}$$

Each small rectangle is a cell, represented by $\Delta_i (i = 1, 2, 3, 4)$. where

$$\begin{aligned} \Delta_1 &: [0, a] \otimes [0, c]; \\ \Delta_2 &: [0, a] \otimes [-d, 0]; \\ \Delta_3 &: [-b, 0] \otimes [-d, 0]; \\ \Delta_4 &: [-b, 0] \otimes [0, c]; \end{aligned}$$

In order to achieve balanced and pure bending of the plate, the bending moment and coupling should satisfy the following equation:

$$\begin{aligned} M_{x2} : M_{x1} &= a : b \\ M_{y2} : M_{y1} &= c : d \\ M_{cx} &= M_{x1} + M_{x2} \\ M_{cy} &= M_{y1} + M_{y2} \end{aligned} \quad (3-18)$$

The direction is shown in Figure 2.

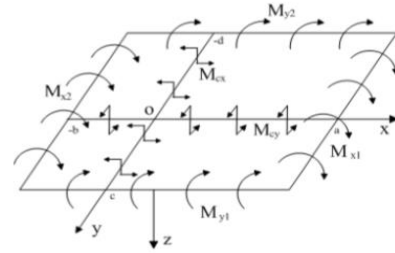


Fig.2 General Case

Therefore, we can get a binary spline as the reflection surface equation of the plate, and the expression on each cell will be:

$$\begin{aligned} \omega_1(x, y) &= b\left(x - \frac{a}{2}\right)^2 - d\left(y - \frac{c}{2}\right)^2 - \frac{1}{4}(ba^2 - dc^2) \\ &= bx^2 - dy^2 - abx + cdy, \quad (x, y) \in \Delta_1, \\ \omega_2(x, y) &= b\left(x - \frac{a}{2}\right)^2 + c\left(y + \frac{d}{2}\right)^2 - \frac{1}{4}(ba^2 - cd^2) \\ &= bx^2 + cy^2 - abx + cdy, \quad (x, y) \in \Delta_2, \\ \omega_3(x, y) &= -a\left(x + \frac{b}{2}\right)^2 + c\left(y + \frac{d}{2}\right)^2 + \frac{1}{4}(ab^2 - cd^2) \\ &= -ax^2 + cy^2 - abx + cdy, \quad (x, y) \in \Delta_3, \\ \omega_4(x, y) &= -a\left(x + \frac{b}{2}\right)^2 - d\left(y - \frac{c}{2}\right)^2 + \frac{1}{4}(ab^2 + dc^2) \\ &= -ax^2 - dy^2 - abx + cdy, \quad (x, y) \in \Delta_4, \end{aligned}$$

It can be written as follows

$$\begin{aligned} s(x, y) &:= \omega_1(x, y) + (c+d)(0-y)_+^2 \\ &\quad + (-a-b)(0-x)_+^2 + (-c-d)(y-0)_+^2 \end{aligned} \quad (3-19)$$

Obviously, the results given in the first two subsections are two special cases in general, and in addition, as long as the external bending moment and the coupling acting on the plate, the rectangular partition can be arbitrarily changed or extended in the median plane of the plate. It can maintain balance and produce pure bending.

Based on the above discussion, we can draw the following conclusion: A class of binary splines as equation $s(x, y)$ It is a subspace of $S_2^1(\Delta_{nm})$, corresponding to a purely curved deformed surface that is advanced to the bending combination and coupling, as shown in Figure 2. Under the assumption of a thin plate with small deviations, the spline can be a sufficiently accurate model of pure bending. In addition, the C^1 continuity of the spline corresponds exactly to the continuity of the rotation angle caused by the coupling, while the discontinuity of the second derivative of the surface corresponds to the discontinuity of the bending moments on both sides of the coupled line, and the conformality condition acting on the inner apex corresponds to the uniqueness of the actual deformed surface of the panel.

Since there is no lateral load, i.e. $q = 0$, it is easy to prove that the above splines can satisfy the equilibrium equation (Eq. (3-11)).

4 Spline Surface of Revolution and its Form of Partition

$$r = \sqrt{x^2 + y^2}$$

4.1. Univariate truncated spline

If truncated spline function is defined in the xOz plane and $x \in [0, 4]$, when $x \in [0, 1]$, the expression of the function is $z = x^2$, the remaining three truncated polynomial is

$$(x-1)_+^2, (x-2)_+^2, (x-3)_+^2$$

respectively, and by default, the smoothing cofactor is 1, then truncated spline can be represented as follows:

$$z = x^2 + (x-1)_+^2 + (x-2)_+^2 + (x-3)_+^2 \tag{4-1}$$

The univariate truncated spline function is shown in Fig.3.

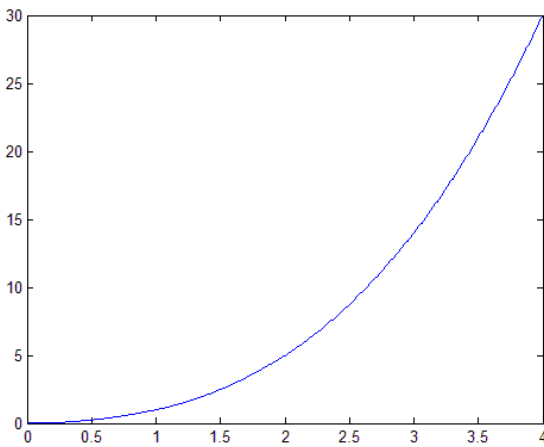


Fig.3 The univariate truncated spline function

4.2. Rotated multivariate spline

4.2.1 Continuous rotated multivariate spline

By rotating Eq. (4-1) around the z-axis, a surface of revolution is obtained. According to the knowledge of analytic geometry, Eq. (4-1) also can be written as follows:

$$z = x^2 + y^2 + \left(\sqrt{x^2 + y^2} - 1\right)_+^2 + \left(\sqrt{x^2 + y^2} - 2\right)_+^2 + \left(\sqrt{x^2 + y^2} - 3\right)_+^2 \tag{4-2}$$

The image of expressions (4-2) is shown in Fig.4.

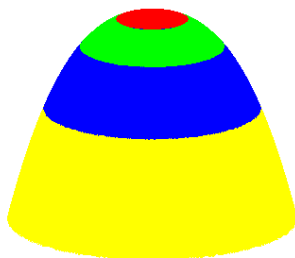


Fig.4 Continuous rotation spline surface

spline function under cylindrical coordinate system is obtained by using coordinate transform to Expression (4-2) as follows:

$$s(r) = z = r^2 + (r-1)_+^2 + (r-2)_+^2 + (r-3)_+^2 \tag{4-3}$$

According to Eq. (4-1), univariate spline function is first-order differentiable, denoted by S_2^1 . And we want to show that the spline of revolution is the S_2^1 -spline. (It is essentially a radial basis function).

Prove: According to Eq. (4-3), equation is as follows:

$$\frac{dz}{dr} = 2r + 2(r-1)_+ + 2(r-2)_+ + 2(r-3)_+ \tag{4-4}$$

where the first derivative is continuous. Making use of the formula of polar coordinates, we have $x = r \cos \theta, y = r \sin \theta$, that is:

$$\partial x = \partial r \cos \theta, \partial y = \partial r \sin \theta \tag{4-5}$$

Then by chain rule, we have

$$\frac{\partial z}{\partial y} = \frac{dz}{dr} \frac{\partial r}{\partial y} = (r + 2(r-1)_+ + 2(r-2)_+ + 2(r-3)_+) \frac{1}{\sin \theta}$$

$$\frac{\partial z}{\partial x} = \frac{dz}{dr} \frac{\partial r}{\partial x} = (r + 2(r-1)_+ + 2(r-2)_+ + 2(r-3)_+) \frac{1}{\cos \theta}$$

Multivariate spline function of the first order partial derivative is continuous when r or θ take a constant value, that is multivariate spline function belongs to S_2^1 .

The partition form of spline surfaces is obtained by projection on xOy plane of the continuous rotation spline, i.e., a class of concentric circles with O is the center and r is the radius. The partition form is shown in Fig.5.

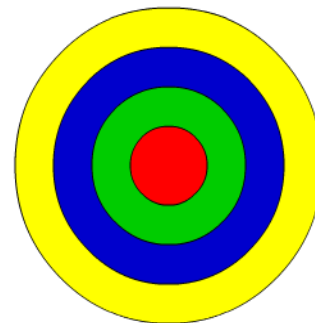


Fig.5 The partition of continuous multivariate spline

Where the circular area with a radius of 4 and a center of $(0,0)$ is multivariate splines located, and partition lines of multivariate splines are a class of circles with radius of 1,2,3, respectively.

4.2.2 Rotation multivariate spline without center

Let

According to Eq. (4-1), spline function in the neighborhood of the point of rotation is an even function, Therefore, when rotating the spline function, we can obtain continuous spline surfaces. Spline surfaces that after rotated will appear a peak near the tip of the point of rotation, if the function in the neighborhood of the point of rotation is not even function. Such an example is given below, truncated spline function defined on xOz plane and $x \in [0, 4]$, where when $x > 2$, there is the original function of $z = x$, the remaining three truncated functions are $(x-1)_+^2, (x-2)_+^2, (x-3)_+^2$ respectively, and we default smoothing cofactor are 1. Hence, truncation spline can be expressed as follows:

$$z = x + (x-1)_+^2 + (x-2)_+^2 + (x-3)_+^2 \quad (4-6)$$

Rotating equation (4-6) along the z axis, we can get the rotation surface as follows:

$$z = \sqrt{x^2 + y^2} + \left(\sqrt{x^2 + y^2} - 1\right)_+^2 + \left(\sqrt{x^2 + y^2} - 2\right)_+^2 + \left(\sqrt{x^2 + y^2} - 3\right)_+^2 \quad (4-7)$$

The image of Expression (4-7) is shown as below:

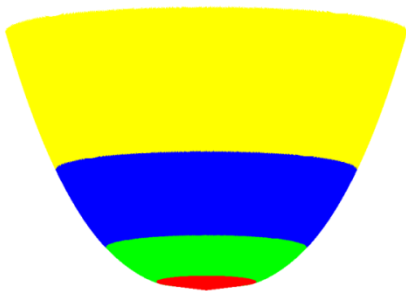


Fig.6 Discontinuous rotation spline

Let $r = \sqrt{x^2 + y^2}$, spline function under cylindrical coordinate system is obtained by using coordinate transform to Expression (4-7) as follows:

$$s(r) = r + (r-1)_+^2 + (r-2)_+^2 + (r-3)_+^2 \quad (4-8)$$

where $r = \sqrt{x^2 + y^2} \leq 1$, the function is conic curve function, therefore, function on a neighborhood of the point of rotation is not smooth. From Fig. 4, we can clearly see a peak generated in the point of rotation. Hence, in the domain $r = \sqrt{x^2 + y^2} \leq 4$, the function is not spline function. But when removed part of the region $r = \sqrt{x^2 + y^2} \leq 1$, a spline surface will obtained in the region of

$$1 < r = \sqrt{x^2 + y^2} \leq 4.$$

Similarly, the partition form of spline surfaces is obtained by projection on xOy plane of the discontinuous rotation spline, i.e., a class of concentric circles with O is the center and r is the radius. The partition form is shown in Fig.7.

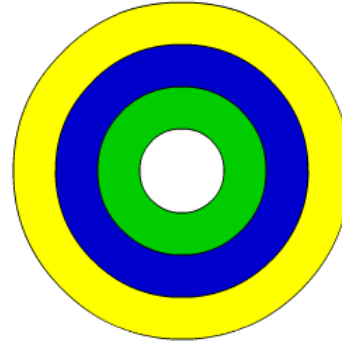


Fig.7 Partition form of discontinuous multivariate spline

As shown in Fig.5, regions bounded by two circles of radius 1 and 4, and the centre point $(0,0)$, are multivariate splines located, and partition lines of multivariate splines are a class of circles with radius of 2 and 3.

4.2.3 Improved rotation multivariate splines

Two of the above rotation multivariate splines, their rotation points are taken at one end of the truncated splines. Continuously rotating splines have good properties, but for those discontinuous splines encountered some problems in their discontinuities. In order to solve the problem of discontinuity, we adjusted the point of rotation of the spline, that is from the end of the truncated spline to the rotation point outside the spline function domain. For example, we shorten the domain of Eq.(4-6) to $x \in [1/2, 4]$, thus under other conditions remain unchanged, the rotation spline surface as shown in the figure below:

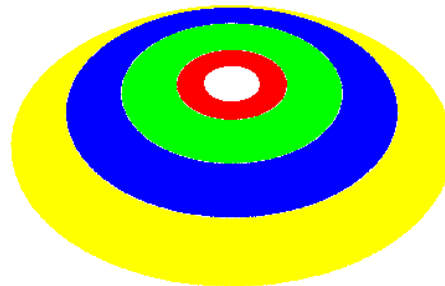


Fig.8 Improved rotation splines

whose partition form is similar to Fig. 7.

Improved rotation spline surfaces are defined on a hollow circular

domain, which overcome the problem of domain narrowed caused by the peak. So that we get the spline surfaces are more universal.

5 Smoothing Cofactor Method on the Circular Domain

5.1 Sectorial partition by concentric circles and rays

There are two parameters $r, \theta \sqrt{a^2 + b^2}$ under the cylindrical coordinate system, but the spline surfaces in above formula (4-3) and (4-8) are r function.

In this section, in order to do a more detailed study on multivariate splines under the cylindrical coordinate system, given new forms of partition, such that the spline surfaces can be written into expressions in terms of r and θ , denoted by $s(r, \theta) \in S_k^u(\Delta_{mn})$, where n is the partition number in r , m is the partition number in θ , k is the degree of spline function, u is the smoothness of the spline.

Using concentric circles and rays to divide the ring through the center, our partitioned form looks like this:

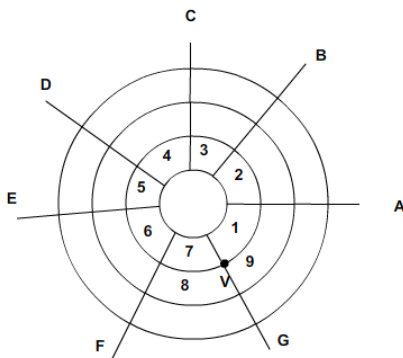


Fig.9 Spline partition by concentric circles

Given an annular domain is $1 \leq r \leq 4$, where partition lines are the rays A, B, C, D, E, F, G , which through the center of a circle and l_1, l_2 represent the circles of radii 2 and 3 respectively, the source of spline function is labeled 1, the flow directions to move forward sequentially, and V is the interior point of partition.

In Fig.9, regions of 1,7,8,9 constitute a star-shaped domain. Four interior edges through V are

$$\begin{aligned} G_{17}(r, \theta) &= \theta - \theta_i = 0 \\ l_{78}(r, \theta) &= r - r_i = 0 \\ G_{89}(r, \theta) &= \theta - \theta_i = 0 \\ l_{91}(r, \theta) &= r - r_i = 0 \end{aligned}$$

respectively. Denote by

$$q_{17}(r, \theta), q_{78}(r, \theta), q_{89}(r, \theta), q_{91}(r, \theta),$$

the smoothing co-factors over the corresponding four interior edges

of the function $s(r, \theta) \in S_k^u(\Delta_{mn})$.

According to the conformality condition at V , we have

$$(q_{17} + q_{89})(\theta - \theta_i)^{u+1} + (q_{78} + q_{91})(r - r_i)^{u+1} = 0 \quad (5-1)$$

Case 1 If $u \leq (k-2)/2$, because of $(\theta - \theta_i)^{u+1}$ and $(r - r_i)^{u+1}$ are relatively prime, $t_1(r, \theta)$ and $t_2(r, \theta)$ exist, which leads to

$$\begin{aligned} (q_{17} + q_{89}) &= (r - r_i)^{u+1} \cdot t_1, \\ (q_{78} + q_{91}) &= (\theta - \theta_i)^{u+1} \cdot t_2 \end{aligned}$$

thus we have

$$t_1(r, \theta) = -t_2(r, \theta). \quad (5-2)$$

Case 2 If $u > (k-2)/2$, we have

$$\begin{aligned} q_{17}(r, \theta) + q_{89}(r, \theta) &= 0, \\ q_{78}(r, \theta) + q_{91}(r, \theta) &= 0. \end{aligned}$$

Through the above derivation, we get the relation among the smooth factors.

By theorem 3, we generalize the partition on circular domain, therefore, the expression of spline

Function $s(r, \theta) \in S_k^u(\Delta_{mn})$ is

$$\begin{aligned} s(r, \theta) &= p(r, \theta) + \sum_{i=1}^m b_i(r, \theta)(\theta - \theta_i)_+^{u+1} \\ &\quad + \sum_{j=1}^n b_j(r, \theta)(r - r_j)_+^{u+1} \\ &\quad + \sum_{i=1}^m \sum_{j=1}^n d_i(r, \theta)(\theta - \theta_i)_+^{u+1} \cdot (r - r_j)_+^u \end{aligned}$$

5.2 Partition by spiral lines and rays

In addition to the above mentioned concentric circles and rays, you can also use spiral lines and rays to carry out the partition for the given circular region. The results obtained are very similar.

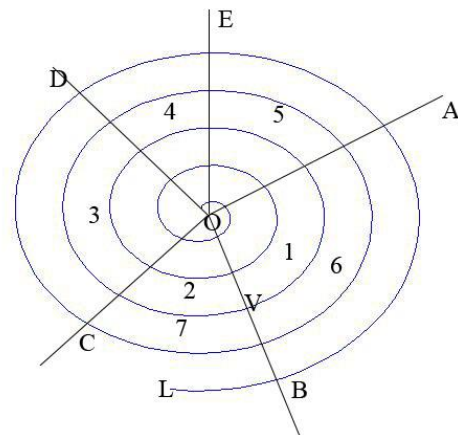


Fig.10 Partition by spiral lines

There is a spiral line in the given region, where partition lines are the rays A, B, C, D, E , which through the center of a circle, and the source of spline function is labeled 1, the flow directions to move forward sequentially, and V is the interior point of partition.

The partition by spiral lines and concentric circles has a very similar form. The representation forms in the whole modelling region only have source function and ray equation under the condition of satisfying conformality condition at nodes. This makes some special surface modeling be easily expressed under the partition by spiral lines.

6 Conclusion

Rotation spline surfaces are obtained by rotating univariate truncated spline function. It overcomes the disadvantage of spline curves and surfaces can not represent any conical surface, provides a good styling tool of the surface design. There is a certain relationship in some way between rotation spline surface and circular plate of the shell theory. It is helpful for us to study mechanical background of circular thin plate. The promotion of spline partition can represent more complex spline surfaces, which is significant to the design of complex surfaces.

7 Acknowledgments

This work was supported by the National Science Foundation of China(51674121,61702184),the Returned Overseas Scholar Funding of Hebei Province(C2015005014) the Hebei Key Laboratory of Science and Applications, and Tangshan Innovation Team Project(18130209B).

8 References

- [1] Schoenberg I J. Contributions to the problem of approximation of equidistant data by analytic functions. *Quart. Appl. Math.*, 1946, 4:49-99, 112-141.
- [2] de Boor C, DeVore R. Approximation by smooth multivariate splines[J]. *Trans. Amer. Math. Soc.*, 1983, 76:775-788.
- [3] Wang Ren-hong. Multiple spline structure and interpolation. *Mathematical Journal*, 1975, 1(2):91-106.
- [4] Wang Ren-hong, Shi Xi-quan, Luo Zhong-yi, Su Zhi-xun. *Multivariate spline functions and their applications*. Beijing: Science Press, 1994.
- [5] Duchon J. Splines Minimizing Rotation-Invariant Semi-Norms in Sobolev Spaces. in: Schempp W, Zeller K (eds.) *Constructive Theory of Functions of Several Variables*. 1976:85-100.
- [6] Wang Ren-hong, Chang Jin-cai. A Kind of Bivariate Spline Space Over Rectangular Partition and Pure Bending of Thin Plate[J]. *Applied Mathematics and Mechanics*, 2007, 28(7):963-971.
- [7] Wang Ren-hong, Chang Jin-cai. The Mechanical Background of Bivariate Spline Space[J]. *Journal of Information and Computational Science*, 2007, 4(1): 299-307.
- [8] Wang Ren-hong, Chang Jin-cai. Bivariate Splines and Golden Section Based on the Theory of Elasticity[J]. *Journal of Mathematics Research and Exposition*, 2011, 31(1): 1-11.
- [9] Wu Zong-min, Su Yang-feng. *Numerical approximation* [M]. Beijing: Science Press, 2008
- [10] Wu Zong-min, *Method and Theory of Scattered Data Fitting* [M]. Beijing: Science Press, 2007
- [11] Wang Shan-shan, Zhang Lu-ming. Split-step orthogonal spline collocation methods for nonlinear Schrödinger equations in one, two, and three dimensions. *Applied Mathematics and Computation*, Volume 218, Issue 5, 1 November 2011, Pages 1903-1916.
- [12] Bai Dong-mei, Zhang Lu-ming. Numerical studies on a novel split-step quadratic B-spline finite element method for the coupled Schrödinger-KdV equations. *Communications in Nonlinear Science and Numerical Simulation*, Volume 16, Issue 3, March 2011, Pages 1263-1273.

- [13] Premaratne, M. Split-step spline method for modeling optical fiber communications systems. *IEEE Photonics Technology Letters*, v 16, n 5, p 1304-6, May 2004.
- [14] Weggel, David C. Properties and dynamic behavior of glass curtain walls with split screw spline mullions. *Journal of Structural Engineering*, v 133, n 10, p 1415-1425, 2007.
- [15] Premaratne, Malin. Split-step spline method for modeling optical fiber communications systems. *IEEE Photonics Technology Letters*, v 16, n 5, p 1304-1306, May 2004.
- [16] Chen Z.C. Khan M.A. Piecewise B-spline tool paths with the arc-Length parameter and their application on high feed, accurate CNC milling of free-form profiles. *Journal of Manufacturing Science and Engineering*, v 134, n 3, p 031007 (13 pp.), June 2012.
- [17] Boris Kvasov. Parallel mesh methods for tension splines. *Journal of Computational and Applied Mathematics*, Volume 236, Issue 5, 1 October 2011, Pages 843-859.
- [18] C.K. Chui, G. Hecklin, G. Nürnberger, F. Zeilfelder. Optimal Lagrange interpolation by quartic image splines on triangulations. *Journal of Computational and Applied Mathematics*, Volume 216, Issue 2, 1 July 2008, Pages 344-363.
- [19] R.K. Mohanty, Jyoti Talwar. SWAGE algorithm for the cubic spline solution of nonlinear viscous Burgers' equation on a geometric mesh. *Results in Physics*, Volume 3, 2013, Pages 195-204.
- [20] Zerroukat, M. Staniforth, A.; Wood, N. The monotonic Quartic Spline Method (QSM) for conservative transport problems. *Journal of Computational Physics*, v 229, n 4, p 1150-66, 20 Feb. 2010.
- [21] Kang Hong-mei, Chen Fa-lai, Deng Jian-song. Modified T-splines. *Computer Aided Geometric Design*, Volume 30, Issue 9, December 2013, Pages 827-843.
- [22] He Yu-xuan, *Finite Element Method based Boundary Loads Computation for Structure Fracture Analysis* [D]. Zhejiang University, 2018.
- [23] W.J. Wu, Parametric Lyapunov Equation Approach to Stabilization and Set Invariance Conditions of Linear Systems with Input Saturation. *International Journal of Applied Mathematics in Control Engineering*, 2018. 1(1): p. 79-84.
- [24] R. Peng, Cheng L., Dai Y., Zhao X., Wu H., and Chen Y., Design and Implementation of Monocular Vision SLAM for Mobile Robot Based on ROS. *International Journal of Applied Mathematics in Control Engineering*, 2018. 1(1): p. 85-91.
- [25] H. Liu, Lv X., and Xiao J., The Research Status and Prospect of Particle Swarm Optimization Algorithm for Water Environment Quality Assessment. *International Journal of Applied Mathematics in Control Engineering*, 2018. 1(1): p. 23-30.
- [26] S. Shi, Liu M., and Ma J., Fractional-Order Sliding Mode Control for a Class of Nonlinear Systems via Nonlinear Disturbance Observer. *International Journal of Applied Mathematics in Control Engineering*, 2018. 1(1): p. 103-110.



[27] Tan Jia-wei, The Mechanical Meaning of Bernstein Basis Function. *International Journal of Applied Mathematics in Control Engineering*, 2018. 1(1): p. 47-54.

Jincai Chang received his B.Sc. degree in 1996 from Ocean University of China, received his M.Sc. degree in 2005 from Yanshan University, and received his Ph.D. degree in 2008 from Dalian University of technology, now he is Professor in North China University of Science and technology. His main research interests include theories and numerical in mathematical modelling and scientific computation, numerical approximation and computational geometry, etc.



Mengyao Bao received her Bachelor's degree in Computational mathematics from North China University of Science and Technology, Tangshan, China, in 2018. She is currently pursuing the MS degree in Computational mathematics at North China University of Science and Technology. Her research is B-spline and parameterization.



Yafei Zhu received a Bachelor's degree in applied mathematics from Hebei North University and is now a graduate student in computational mathematics in North China University of Science and Technology. In the past four years, she has taken several specialized courses, including numerical analysis. Her research fields include radial basis function neural network, B-spline and so.



Yajing Qi received a Bachelor's degree in applied mathematics from Hebei North University and received master's degree from North China University of Science and Technology. Her research is B spline and so on. Now she works for education.



Xiaolong Zhang is a PhD student at School of Mechanical Engineering, Jiangsu University, Zhejiang, China. His main research is spline, peridynamic waves and ultrasonic detect. He has participated in projects of the National Natural Science Foundation of China and Postgraduate Research & Practice Innovation Program of Jiangsu Province.

